

Stat3 signaling in acute myeloid leukemia: ligand-dependent and -independent activation and induction of apoptosis by a novel small-molecule Stat3 inhibitor

Michele S. Redell,¹ Marcos J. Ruiz,¹ Todd A. Alonzo,^{2,3} Robert B. Gerbing,³ and David J. Tweardy⁴

¹Texas Children's Cancer Center, Baylor College of Medicine, Houston, TX; ²University of Southern California Keck School of Medicine, Los Angeles, CA;

³Children's Oncology Group, Arcadia, CA; and ⁴Department of Medicine, Baylor College of Medicine, Houston, TX

Acute myeloid leukemia (AML) is an aggressive malignancy with a relapse rate approaching 50%, despite aggressive chemotherapy. New therapies for AML are targeted at signal transduction pathways known to support blast survival, such as the Stat3 pathway. Aberrant activation of Stat3 has been demonstrated in many different malignancies, including AML, and this finding is frequently associated with more aggressive disease. The objectives of this study were: (1) to character-

ize Stat3 signaling patterns in AML cell lines and primary pediatric samples; and (2) to test the efficacy and potency of a novel Stat3 inhibitor in inducing apoptosis in AML cells. We found that Stat3 was constitutively activated in 6 of 7 AML cell lines and 6 of 18 primary pediatric AML samples. Moreover, constitutively phosphorylated Stat3 was frequent in samples with normal karyotype but uncommon in samples with t(8;21). Most cell lines and primary samples responded to G-CSF

stimulation, although the sensitivity and magnitude of the response varied dramatically. Our novel small-molecule Stat3 inhibitor, C188-9, inhibited G-CSF-induced Stat3 phosphorylation, induced apoptosis in AML cell lines and primary samples, and inhibited AML blast colony formation with potencies in the low micromolar range. Therefore, Stat3 inhibition may be a valuable strategy for targeted therapies for AML. (*Blood*. 2011;117(21):5701-5709)

Introduction

Stat3 is a critical signaling intermediate in hematopoietic cells that is activated by recruitment to tyrosine-phosphorylated receptor complexes, including the granulocyte colony-stimulating factor (G-CSF) receptor. Recruitment leads to phosphorylation of Stat3 on tyrosine 705 (pY705), tail-to-tail dimerization, nuclear accumulation, and gene transcription. Recruitment and dimerization require interactions between the Stat3 Src homology 2 (SH2) domain and pY peptide motifs located within receptor complexes or within Stat3, respectively. Stat3-responsive genes include antiapoptosis genes, cell cycle regulators, and angiogenesis factors. Gene activation is enhanced by S727 phosphorylation and appears to be required for accumulation of Stat3 within mitochondria, where it promotes oxidative phosphorylation.¹

The evidence that Stat3 signaling plays a key role in cancer was first obtained from cells transformed by the oncogene *v-src*.² Subsequently, several other oncoproteins that activate tyrosine kinase pathways were shown to result in constitutive Stat3 activation.³ Fibroblasts expressing a constitutively active Stat3 mutant (Stat3-C) developed malignant properties in culture and formed tumors in nude mice.⁴ Clinically, constitutively active Stat3 was first demonstrated in squamous cell carcinoma of the head and neck⁵ and since has been demonstrated in many different cancers, including acute myeloid leukemia (AML),⁶⁻⁸ although notably no studies have been done with pediatric patients. As in other malignancies, the finding of constitutive Stat3 activity in AML is associated with poor prognosis,⁶ possibly as a result of increased resistance to chemotherapy. Indeed, recent studies have demonstrated that acquired resistance to tyrosine kinase inhibitors (TKI) can be attributed in

some cases to increased activity of the Stat3 pathway, and Stat3 inhibition restores TKI sensitivity.^{9,10}

Given that Stat3 activity is an important factor in malignant behavior and chemoresistance, a variety of approaches have been undertaken to target Stat3. Such studies consistently have shown the ability to reduce tumor cell growth in vitro and in xenograft models. Most of the work targeting Stat3 has focused on epithelial cancers, whereas therapeutic targeting strategies for AML have been directed at tyrosine kinases, including Src, Flt3, and c-kit. Certainly small-molecule TKIs, such as imatinib mesylate and other newer drugs, have proven remarkably effective in many cases; nevertheless, resistance remains a difficult problem. Therefore, new approaches for blocking signaling pathways are needed. Stat3 is an attractive target because the protein itself is not mutated, but rather it mediates abnormal signaling because of a variety of different upstream genetic and/or epigenetic changes.

In this study, we report the prevalence of constitutive and G-CSF-induced tyrosine-phosphorylated Stat3 in a panel of AML cell lines and a cohort of primary pediatric AML samples, and the effects of Stat3 inhibition on AML cell growth and survival. We recently identified 3 small-molecule probes (C3, C30, and C188) that target the phosphotyrosine (pY) peptide binding site within the Stat3 SH2 domain,¹¹ thereby blocking both recruitment to tyrosine kinase-containing complexes and dimerization. Subsequently, we identified second-generation Stat3 inhibitors based on the scaffold of C188. Here we report that one of these small molecules, C188-9, inhibited ligand-induced Stat3 phosphorylation with a log-fold improvement in efficacy in AML cell lines compared with C188, induced apoptosis in AML cell lines and primary pediatric AML

Submitted April 16, 2010; accepted March 8, 2011. Prepublished online as *Blood* First Edition paper, March 29, 2011; DOI 10.1182/blood-2010-04-280123.

The publication costs of this article were defrayed in part by page charge payment. Therefore, and solely to indicate this fact, this article is hereby marked "advertisement" in accordance with 18 USC section 1734.

The online version of this article contains a data supplement.

© 2011 by The American Society of Hematology

samples, and inhibited colony formation by primary AML cells. Therefore, aberrant Stat3 signaling is probably an important element in AML cell survival and chemoresistance. Further development of drugs targeting Stat3 may be of tremendous benefit for patients with this devastating disease.

Methods

Cell lines

Kasumi-1 and GDM-1 cell lines were purchased from ATCC. HL-60, KG-1, and THP-1 cell lines were gifts of Dr Terzah Horton (Baylor College of Medicine, Houston, TX). NB-4 cells were a gift of Dr Shuo Dong (Baylor College of Medicine, Houston, TX). K562 cells were provided by the Baylor College of Medicine Tissue Culture storage facility. HL-60 and K562 cell lines were maintained in IMDM (HyClone) with 10% FBS (Invitrogen), 100 units/mL penicillin and 100 μ g/mL streptomycin (Pen/Strep; Invitrogen). KG-1 cells were maintained in IMDM with 20% bovine growth serum (HyClone) and Pen/Strep. The other cell lines were maintained in RPMI (ATCC) with 10% FBS and Pen/Strep. All cells were grown in a humidified, 37°C incubator with 5% CO₂.

Primary AML samples

Twenty primary AML samples were obtained from the Children's Oncology Group (COG) AML Reference Laboratory (Dr Soheil Meshinchi, University of Washington). These samples were derived from pediatric patients with de novo AML who were treated on protocols CCG 2891, CCG 2961, or AAML03P1 and gave written informed consent, in accordance with the Declaration of Helsinki, for banking of bone marrow for future research. Mononuclear cells were enriched by density centrifugation and cryopreserved. After thawing, samples were incubated in serum-free medium (StemSpan H3000; StemCell Technologies) for 2 hours before analysis. Of the 20 original samples, 1 was excluded for low viability after thawing, and another was excluded for a diagnosis of myelodysplastic syndrome.

An additional 13 samples from 8 patients were obtained from the Research Tissue Support Service of Texas Children's Cancer Center and were used for the Stat3 inhibitor studies. These were obtained from pediatric AML patients who were treated at Texas Children's Cancer Center and gave written informed consent, in accordance with the Declaration of Helsinki, for remainder bone marrow to be stored for research. Mononuclear cells were enriched by density centrifugation and cryopreserved. Bone marrow mononuclear cells from normal donors were obtained by rinsing leftover cells from the collection filter. As with the AML samples, mononuclear cells were enriched by density centrifugation and cryopreserved. These studies were approved by the Institutional Review Board of Baylor College of Medicine.

Antibodies and drugs

FACS antibodies were purchased from BD Biosciences and included PE anti-pY705-Stat3 and PE isotype control. Primary antibodies for Western blotting included anti-pY705-Stat3 (Cell Signaling Technology) and anti-Stat3 (BD Transduction Laboratories); anti-pT202/pY204-ERK1/2 and anti-ERK1/2 (p42/44; Cell Signaling Technology); anti-pS473-Akt and anti-Akt (Cell Signaling Technology); and anti- β -actin (Abcam). Secondary antibodies included horseradish peroxidase-conjugated anti-mouse Ig (Invitrogen); IRDye 700DX-conjugated anti-mouse and anti-rabbit Ig (LI-COR Biosciences); and IRDye 800-conjugated anti-mouse and anti-rabbit Ig (Rockland Immunochemicals).

Recombinant human G-CSF (Neupogen Filgrastim; Amgen) was diluted in PBS or IMDM before use. C188 (#7917648; ChemBridge, www.hit2lead.com) and 188-9 (#F1113-0789; Life Chemicals, www.lifechemicals.emolecules.com) were purchased. Both were reconstituted at 20mM in DMSO and then further diluted in sterile water or IMDM just before use. Stock solutions were stored at 4°C protected from light.

FACS analysis of phospho-Stat3

Cell lines were washed and replated at 5 to 10 \times 10⁵ cells/mL in IMDM or RPMI without serum for 2 hours. Primary cells were plated in serum-free StemSpan H3000. Cells were either stimulated with G-CSF for 15 minutes or remained unstimulated. Cells were then fixed in 2% paraformaldehyde at 37°C for 10 minutes, pelleted, washed once in flow buffer (PBS, pH 7.2, with 0.2% BSA and 0.09% sodium azide), and permeabilized in 100% ice cold methanol, on ice for 30 minutes. Cells were washed twice in flow buffer and then labeled with anti-pY705-Stat3-PE or isotype control for 20 minutes. Cells were washed once in flow buffer and analyzed on a FACScan (BD Biosciences). CellQuest Version 3.3 (BD Biosciences) was used for data acquisition and analysis. Further analysis was carried out with FlowJo Version 7.5 (TreeStar).

For experiments using the Stat3 inhibitors, cells were pretreated with the drug for 1 hour at 37°C before G-CSF. Control samples were treated with a concentration of DMSO equal to the DMSO concentration of the highest dose of compound used in the assay (0.15%-0.5%).

Western blotting

Cell lines and primary samples were treated with C188-9 and G-CSF as described in the preceding paragraph. After 15 minutes of G-CSF stimulation, cells were pelleted and lysed in NP-40 lysis buffer (20mM Tris, pH 8.0, 140mM NaCl, 10% glycerol, 1% NP-40, 2mM EDTA). Protease inhibitors, including Protease Inhibitor Cocktail (P2714; Sigma-Aldrich) and 1mM phenylmethylsulfonyl fluoride, and a phosphatase inhibitor cocktail (PhosSTOP; Roche) were added just before use. Protein was quantified with the Bio-Rad protein assay.

Whole cell lysates were separated by SDS-PAGE and then transferred to polyvinylidene difluoride membranes. Primary antibody was incubated on the membrane overnight at 4°C. Secondary antibody was incubated on the membrane for 1 hour at room temperature. In most cases, reactions were detected using Pierce ECL Western Blotting Substrate (Thermo Scientific). The ERK and AKT blots were incubated with an IRDye-conjugated secondary antibody, and bands were directly detected on an Odyssey Infrared Imaging System (LI-COR Biosciences).

Densitometry analysis was done with Image J (National Institutes of Health [NIH], <http://rsb.info.nih.gov/ij/>). Each Stat3 densitometric value was normalized to the corresponding β -actin value. To account for differences in exposures between blots, each normalized Stat3 value from an AML sample was divided by the normalized Stat3 value from KG-1 lysate run on the same gel.

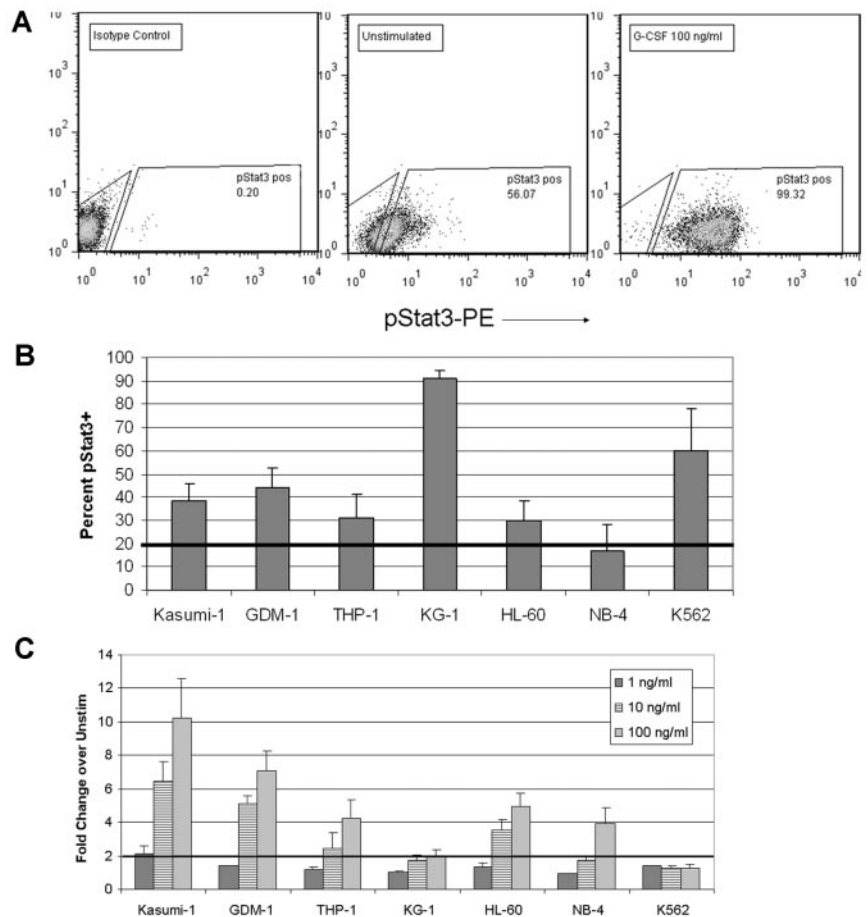
Tyrosine kinase array

Kasumi-1 and THP-1 cells were stimulated with G-CSF (100 ng/mL) for 15 minutes with or without pretreatment with C188-9 (10 μ M) for 1 hour. Whole cell lysates (1 mg per membrane) were incubated with the array membranes, followed by biotinylated anti-pY and streptavidin-horseradish peroxidase, according to the manufacturer's instructions (Ray Biotech). Spot densities were quantified with Image J (NIH, <http://rsb.info.nih.gov/ij/>).

Quantitative RT-PCR

Cell lines were incubated with 10 μ M C188-9 for 1 hour and then stimulated with G-CSF (100 ng/mL) for 1 hour. Control experiments were performed with NB-4 cells using all-*trans* retinoic acid (ATRA; 1 μ M; Sigma-Aldrich) in place of G-CSF. Control aliquots were uninhibited and unstimulated. Total RNA was extracted using the RNeasy Plus kit (QIAGEN), and 500 ng was used in a reverse transcriptase reaction to generate cDNA (MultiScribe; Applied Biosystems) for the template in quantitative real-time PCR reactions (ABI Prism 7300; Perkin Elmer–Applied Biosystems). Gene-specific TaqMan primer/probe sets for *SOCS3* (Hs02330328_s1; Applied Biosystems), *PIMI* (Hs01065498_m1), and *CCL24* (Hs00171082_m1) were purchased. Parallel reactions were performed for 18S rRNA, using 5 ng RNA (18S primer/probe kit; Applied Biosystems). The fold change in mRNA was calculated by the $\Delta\Delta C_t$ method.¹²

Figure 1. Stat3 phosphorylation is constitutive and inducible in AML cell lines. (A) Representative dot plot illustrating the gating scheme used for analysis of pStat3 by FACS. The first gate is set to include cells and exclude debris based on forward and side scatter properties (not shown). The pStat3⁻ and pStat3⁺ gates are based on the isotype control-stained sample (left). The percentages of constitutive and inducible pStat3⁺ cells are determined for unstimulated cells (middle) and cells treated with 100 ng/mL G-CSF for 15 minutes (right), respectively. (B) The percentage of pStat3⁺ cells in the unstimulated condition is shown for all 7 AML cell lines evaluated. Values are mean \pm SEM for 5 or more replicates. (C) The fold change in the MFI of cells after stimulation with the indicated dose, compared with the unstimulated cells, is shown for the AML cell lines. A response to G-CSF was defined as an increase of at least 2-fold. Values are mean \pm SEM for 2 to 5 replicates.



Apoptosis assays

Cell lines were plated at 2 to 5×10^5 cells/mL in growth medium and treated with increasing doses of inhibitor for 24 hours. Primary samples were enriched for CD34⁺ cells by labeling with anti-CD34-conjugated microbeads (Human CD34 Microbead Kit; Miltenyi Biotec) followed by immunomagnetic sorting (AutoMACS Pro; Miltenyi Biotec). CD34⁺ AML cells were plated at 1 to 2×10^5 cells/mL in IMDM with 20% FBS and Pen/Strep, and incubated with C188-9 for 48 hours. Cells were then harvested and labeled using the PE Annexin V Apoptosis Detection Kit (BD Biosciences Pharmingen). Analysis was carried out on a FACScan with CellQuest software Version 3.3 (BD Biosciences). The fraction of spontaneous apoptosis was determined from an untreated sample and then subtracted from the drug-treated samples to yield the percentage of apoptosis attributed to drug treatment.

Methylcellulose colony assays

Unselected, untreated primary AML samples were plated in Methocult H4434 methylcellulose medium containing SCF, GM-CSF, IL-3, and erythropoietin (StemCell Technologies) at 10^5 cells/dish, in duplicate dishes per condition. Increasing concentrations of C188-9 were added directly to the medium at the same time that the cells were added. Pen/Strep was also added. Dishes were incubated in a humidified incubator at 37°C. Colonies containing at least 30 cells were counted after 12 to 15 days.

Statistics

For the in vitro drug studies, dose-response curves were generated and 50% inhibitory concentration/50% effective concentration (IC_{50}/EC_{50}) values estimated by 4-parameter logistic equation (model 205, XLFit 4.2). Linear regression analysis for the correlation of constitutive phosphorylated Stat3 (pStat3) with total Stat3 was performed with SPSS Version 17.

Results

Stat3 phosphorylation was both constitutive and inducible in most AML cell lines

We used phosphoflow to determine the degree and frequency of tyrosine-pStat3, and the sensitivity of Stat3 activation to G-CSF stimulation, in a panel of human AML cell lines. Cells were treated with G-CSF at doses of 1, 10, or 100 ng/mL for 15 minutes. Parallel aliquots remained unstimulated for the determination of constitutive pStat3. As shown in Figure 1, constitutively phosphorylated Stat3 was detected at various levels in all 7 cell lines. The cell lines were variable in their sensitivities to G-CSF-induced Stat3 phosphorylation. With a G-CSF response defined as a 2-fold or more increase in the mean fluorescence intensity (MFI) over unstimulated cells, 6 of the 7 cell lines were responsive to at least the highest dose of G-CSF (100 ng/mL). Although K562 cells (CML blast crisis) demonstrated a high level of constitutive pStat3, attributable to activity of the BCR-Abl fusion kinase,^{13,14} these cells were unresponsive to G-CSF at all doses. Four of the 7 cell lines responded to the 10 ng/mL dose of G-CSF, and only Kasumi-1 cells responded to 1 ng/mL G-CSF. The immunoreactivity for pStat3 in stimulated and unstimulated cells reflected specific detection of pStat3, rather than nonspecific binding, because preincubation of the anti-pStat3 antibody with the immunizing peptide (generous gift of BD Biosciences) reduced the pStat3-PE signal nearly to the level of the isotype control reaction (supplemental Figure 1, available on the *Blood* Web site; see the Supplemental

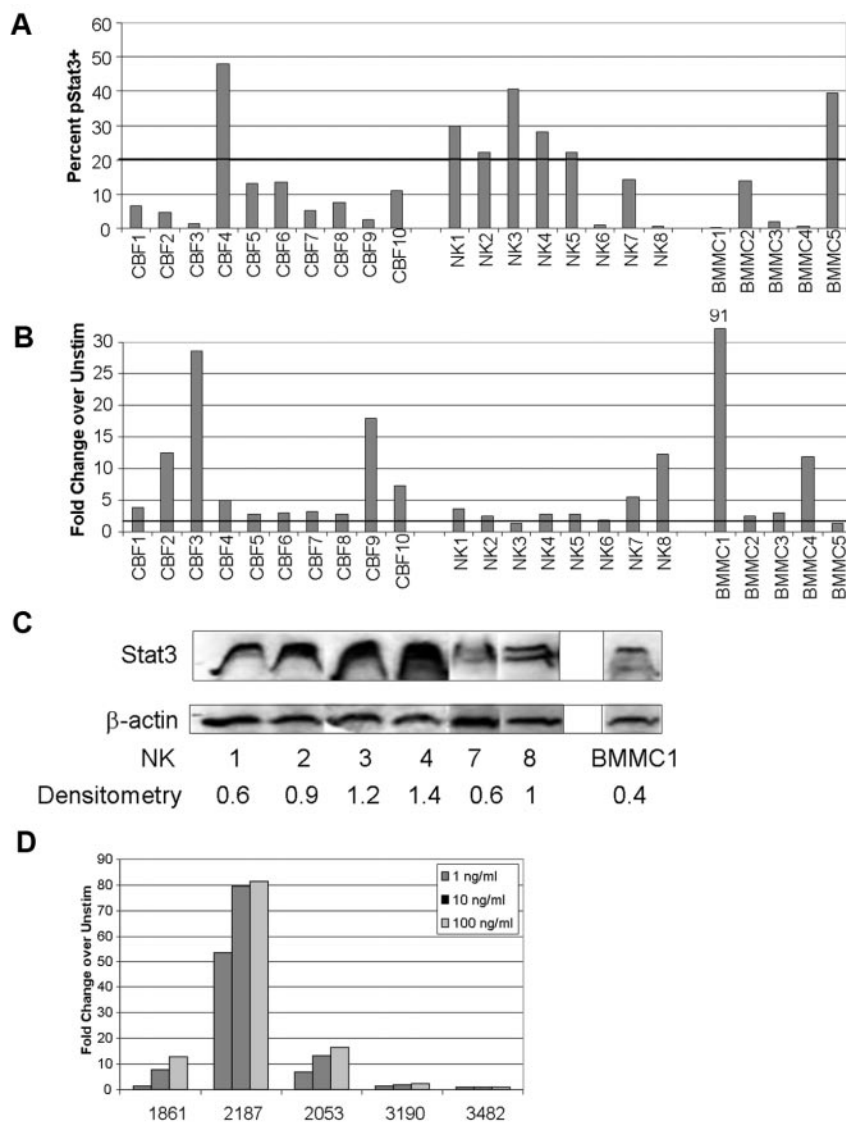


Figure 2. Stat3 phosphorylation is constitutive and inducible in primary pediatric AML samples and correlates with survival. (A) Primary AML samples from the COG AML Reference Laboratory were analyzed by FACS for pStat3. The percentage of pStat3⁺ events in the unstimulated condition is shown. Samples with more than or equal to 20% of pStat3⁺ cells were considered to have constitutive Stat3 activation. BMNCs are from normal donors. (B) The fold change in the percentage of pStat3⁺ cells after stimulation with 100 ng/mL G-CSF, compared with the unstimulated cells, is shown for the 18 primary AML samples from COG and the 5 normal control samples. (C) Total Stat3 protein levels for the NK samples and selected normal BMMC samples were measured by Western blot. The band density for each Stat3 band (including Stat3 α/β doublets) was normalized to the corresponding β -actin band density. This value was then divided by the normalized density for a KG-1 sample run on the same gel (not shown) to adjust for differences in exposures between gels. The adjusted densitometry values for each band are shown at the bottom. The figure was compiled from nonadjacent lanes and/or separate gels, with the exception of lanes 1 and 2 (samples NK1 and NK2), which were adjacent on the same gel. (D) The fold change for cells stimulated with G-CSF at the indicated doses, compared with unstimulated cells, is shown for 5 primary AML samples obtained from the Texas Children's Cancer Center.

Materials link at the top of the online article). These results show that constitutive pStat3 was very frequent in human AML cell lines and that further activation of Stat3 could be achieved in most cell lines on treatment with a relevant ligand.

Constitutive pStat3 was common in cytogenetically normal primary AML samples

Primary AML samples from pediatric patients enrolled in COG AML treatment studies CCG2891, CCG2961, or AAML03P1 were obtained from the COG AML Reference Laboratory. Cohorts of cytogenetically low-risk (t(8;21), CBF) and intermediate-risk (normal karyotype, NK) patients were evaluated. Patient characteristics are summarized in supplemental Table 1. In addition, 5 samples of bone marrow mononuclear cells (BMNCs) from normal donors were examined. Mean viability of the AML samples after thawing was 74.4% (range, 64%-87%). Because of limited cell numbers in some cases, only the unstimulated and 100 ng/mL G-CSF-stimulated conditions were measured. We chose more than or equal to 20% pStat3⁺ events as the threshold for considering a sample to have constitutive pStat3 because this value approximates the mean \pm SE of 18.6% for pStat3⁺ events in the normal BMMC samples.

We found that 6 of 18 primary AML samples demonstrated more than 20% pStat3⁺ events, with 5 of those in the NK group (Figure 2A). Only 1 of 10 CBF samples demonstrated more than 20% pStat3⁺ cells, as did 1 of the 5 normal control marrow samples. This finding is intriguing, given that a previous study in an adult cohort found that constitutively active Stat3 was associated with a shorter time to relapse.⁶ Further studies are currently underway to determine whether constitutively active Stat3 is significantly associated with cytogenetic features and/or clinical outcome in pediatric patients.

Stat3 phosphorylation occurred in response to G-CSF in most primary AML samples

Most samples (16 of 18) responded to 100 ng/mL G-CSF, including all of the CBF samples and 6 of 8 NK samples (Figure 2B). Likewise, 4 of 5 normal marrow samples responded to G-CSF. To determine whether primary samples demonstrate variable sensitivity to G-CSF, as was shown for the AML cell lines, we studied an additional cohort of 5 primary AML samples obtained from Texas Children's Cancer Center (supplemental Table 2). Similar to the results shown for the AML cell lines, we found wide variability in

the sensitivity of Stat3 phosphorylation to G-CSF (Figure 2D). Two samples had a more than 2-fold response to the lowest dose of G-CSF (1 ng/mL), with sample #2187 demonstrating a dramatic response of more than 50-fold increase in pStat3. Two more samples responded at the 10 ng/mL dose, and the fifth sample (#3482) was unresponsive at all doses. These results confirm the observation made with the AML cell lines: that most, though not all, AML samples activated Stat3 downstream of the G-CSF receptor, and the sensitivity to G-CSF varied greatly.

One means by which the levels of pStat3, both constitutive and inducible, may vary is because of different levels of Stat3 protein expression. For this reason, we measured total Stat3 protein levels by Western blot, for samples with sufficient material. We found that the level of Stat3 expression also varied between samples (Figure 2C), but there was not a significant correlation between the actin-normalized Stat3 band density (Image J; NIH, <http://rsb.info.nih.gov/ij/>) and the percentage of constitutive pStat3⁺ cells ($R = 0.286$; $P = .58$). Therefore, the variation in the levels of constitutive pStat3 in these samples did not depend solely on the overall expression level of the protein.

C188-9 inhibited G-CSF–induced Stat3 phosphorylation

Using a virtual ligand screening approach, our laboratory recently reported the identification of 3 small-molecule probes (C3, C30, and C188) that targeted the pY-peptide binding site within the Stat3 SH2 domain. The compounds competitively inhibited Stat3 binding to its phosphopeptide ligand, thereby blocking ligand-induced Stat3 phosphorylation, but had no effect on ligand-induced Stat1 phosphorylation. These compounds also induced apoptosis of Stat3-dependent, but not Stat3-independent, breast cancer cell lines.¹¹ Of the 3 hits, C188 was the most potent for induction of apoptosis in AML cell lines, with an EC₅₀ of 34.6 μM in Kasumi-1 cells (data not shown). We performed similarity screening using the benzenesulfamide scaffold of C188¹¹ followed by 3-D pharmacophore analysis and identified more potent probes (T. K. Eckols, X. Xu, M. Kasembeli, and D.J.T., manuscript in preparation). One of the most active of these second-generation probes, C188-9, inhibited G-CSF–induced Stat3 phosphorylation with low micromolar potency. For the 6 AML cell lines analyzed, the IC₅₀ values for inhibiting G-CSF–induced pStat3 were quite similar, ranging from 4.1 μM in KG-1 cells to 8.3 μM in NB-4 cells (Figure 3A-B; supplemental Table 3). In some cases, pStat3 intensity even decreased below the level of unstimulated cells (eg, Figure 3A right). Immunoblot analysis confirmed that C188-9 inhibited Stat3 phosphorylation but did not alter the level of total Stat3 protein (Figure 3C).

To determine whether C188-9 could be inhibiting Stat3 phosphorylation by inhibiting an upstream tyrosine kinase, rather than directly interacting with Stat3 as predicted by the modeling data, we analyzed the effect of 10 μM C188-9 on the phosphorylation status of multiple tyrosine kinases, using a protein array (Ray Biotech). In Kasumi-1 cells, only Tie2 kinase was inhibited to less than 50% by C188-9 before treatment, whereas Janus kinases (Jak1, Jak2) and Src family kinases (Hck, Lyn, and Src) were minimally affected (Figure 3D). No affected kinases were noted in THP-1 cells, although fewer kinases were measurable (data not shown). Lastly, to determine whether C188-9 could be inhibiting other important signaling pathways in leukemia cells, we analyzed pERK1/2 (p42/44) and pAKT and saw no effect of the compound on these pathways (Figure 3E).

C188-9 decreased expression of Stat3 target genes and induced apoptosis in AML cell lines

To evaluate the effect of C188-9 on the expression of target genes that are up-regulated by Stat3, AML cell lines were pretreated with 10 μM C188-9 for 1 hour, then stimulated with G-CSF (100 ng/mL) for 1 hour, and total RNA was extracted for quantitative RT-PCR. The *SOCS3* gene is a Stat3 target gene that encodes the Jak inhibitory protein SOCS3. *PIM1* encodes the kinase Pim1, an oncogene implicated in several cancers, including AML,¹⁵ which is also an accepted target gene of Stat3.¹⁶ The mRNA levels for these transcripts were up-regulated in AML cells on G-CSF treatment, and the increase was reduced in cells that were pretreated with C188-9 (Figure 4A). In contrast, C188-9 did not significantly affect the level of the ATRA-inducible transcript *CCL24*¹⁷ in NB-4 cells stimulated with ATRA. The smaller effect of C188-9 on *PIM1* mRNA in Kasumi-1 cells was possibly the result of ERK and/or Akt pathways up-regulating this gene, as has been described.¹⁸ Indeed, Figure 3E shows that ERK1/2 and Akt were dramatically activated in Kasumi-1 cells by G-CSF and not inhibited by C188-9. These studies confirm that C188-9 not only inhibited Stat3 activation, it also inhibited Stat3-dependent gene transcription.

We next evaluated the effect of C188-9 on apoptosis of AML cell lines. Cells were treated with increasing doses of the drug for 24 hours; then apoptotic cells were quantified with annexin V-PE. The EC₅₀ values of the 7 AML cell lines varied between 6 and 8 μM in GDM-1 and Kasumi-1 cells to more than 43 μM in K562 cells (Figure 4B). To confirm that this variability in apoptosis was the result of variable dependence on Stat3 activity and not to variable off-target effects, we performed similar apoptosis studies with JSI-124, which is reported to inhibit Jak and Stat3 phosphorylation, although the binding site is not known.¹⁹ We obtained similar results, with Kasumi-1 cells being among the most sensitive to apoptosis induction by JSI-124, and K562 cells being least sensitive (supplemental Table 4). These results demonstrate that inhibition of Stat3 activity induced apoptosis in AML cell lines.

C188-9 inhibited G-CSF–induced Stat3 phosphorylation and induced apoptosis in primary pediatric AML cells

To determine whether the effects of C188-9 on AML cell lines could also be demonstrated in primary AML cells, we tested samples from Texas Children's Cancer Center (supplemental Table 2). Cells were treated with C188-9 at doses ranging from 0.3 to 10 μM for 1 hour, stimulated with G-CSF for 15 minutes; then pStat3 was measured by FACS. The results for 4 primary AML samples are consistent with the results from the 7 AML cell lines. C188-9 inhibited G-CSF–induced Stat3 phosphorylation in a dose-dependent manner, with IC₅₀ values ranging between 8 and 18 μM (Figure 5A-B).

Next, we determined the ability of C188-9 to induce apoptosis in primary AML samples. To reduce heterogeneity and enrich for leukemia-initiating cells, primary samples underwent immunomagnetic selection for CD34⁺ cells. Cells were plated at 1 to 2 × 10⁵ cells/mL in IMEM with 20% FBS. C188-9 was added to the wells in doses ranging from 0.3 to 100 μM. Cells were treated with C188-9 for 48 hours, and apoptosis was quantified by annexin V staining. All 5 primary samples demonstrated dose-dependent apoptosis, with EC₅₀ values ranging from 0.8 to 25 μM (Figure 5C), confirming that primary AML cells, like cell lines, undergo apoptosis on treatment with C188-9.

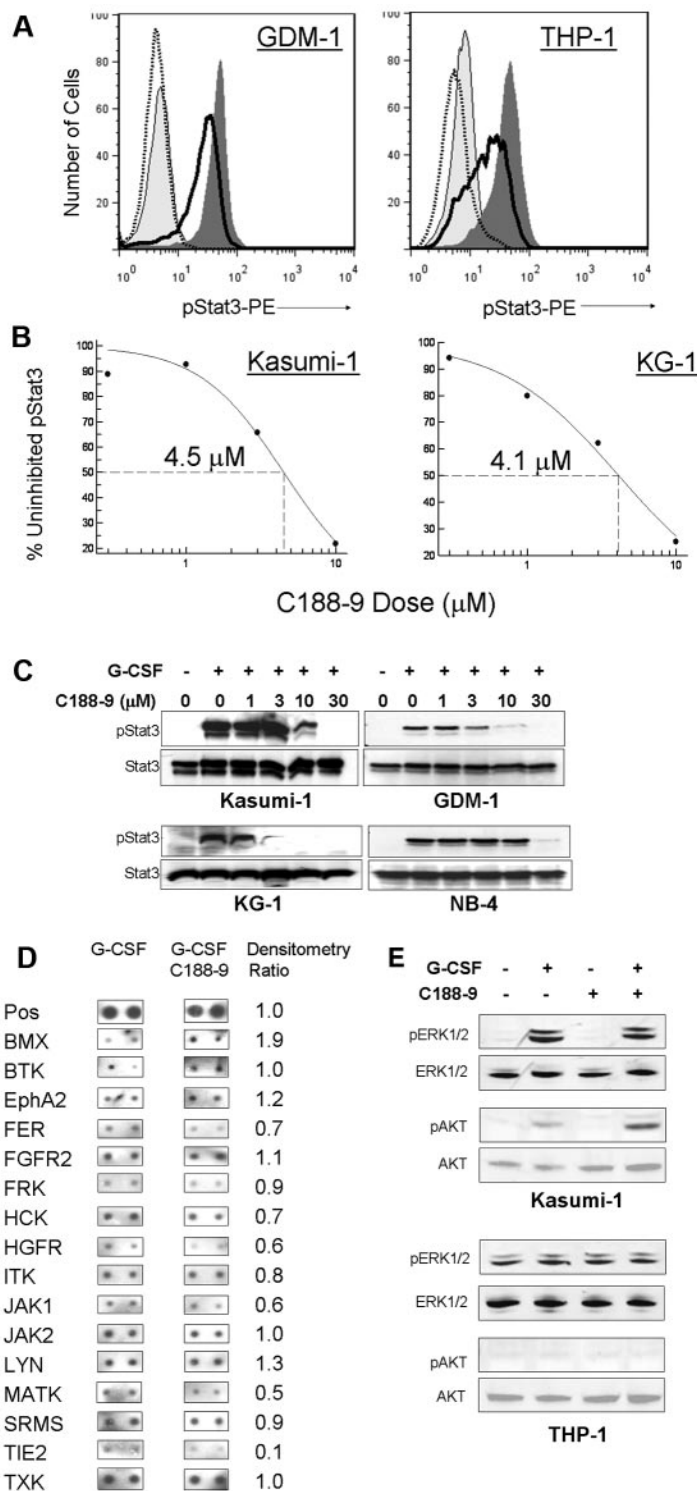


Figure 3. A novel Stat3 SH2 small-molecule probe, C188-9, inhibits Stat3 phosphorylation in AML cells. (A) C188-9 inhibited G-CSF–induced pStat3 in a dose-dependent manner, as demonstrated by FACS. Representative histogram overlays for Kasumi-1 and THP-1 cell lines are shown. Light gray area represents unstimulated; dark gray area, G-CSF (100 ng/mL) only; solid line, G-CSF + 3 μM C188-9; and dotted line, G-CSF + 10 μM C188-9. (B) The dose-response relationship for C188-9 inhibition of G-CSF–induced pStat3 for 4 AML cell lines is shown. The IC₅₀ values for all 6 cell lines were between 4 and 8 μM. Each point represents the mean of at least 3 separate experiments. (C) C188-9 inhibited G-CSF–induced pStat3 in a dose-dependent manner but did not alter total Stat3 protein levels, as demonstrated by Western blotting. For both FACS and Western blotting, cells were treated with C188-9 at the indicated dose for 1 hour and then stimulated with G-CSF (100 ng/mL) for 15 minutes. (D) C188-9 did not affect the tyrosine phosphorylation levels of most tyrosine kinases represented on a tyrosine kinase protein array. Duplicate array spots from cells stimulated with 100 ng/mL G-CSF (left) and cells pretreated with 10 μM C188-9 before G-CSF (middle) are shown. The ratio of inhibitor/no inhibitor densitometric values is shown in the right-most column. (E) C188-9 did not inhibit the activity of the MAPK/ERK pathway or the Akt pathway, as assessed by pERK1/2 and pAkt immunoreactivities.

We also evaluated the effect of C188-9 on the clonogenicity of primary AML cells grown in methylcellulose medium with growth factors (Methocult H4434; StemCell Technologies). C188-9 (0.3–100 μM) was added directly to the methylcellulose at the time of plating. After 14 days in culture, colonies were enumerated, and IC₅₀ values were determined. This assay specifically evaluates the effect of Stat3 inhibition on the subset of AML cells that are capable of self-renewal and/or proliferation. All 5 primary AML

samples evaluated in this assay had IC₅₀ values for inhibition of colony formation less than 10 μM, ranging from 0.4 to 8.4 μM (Figure 5D). DMSO alone had a negligible effect in most cases (data not shown). We performed similar colony-forming unit (CFU) assays with 4 normal human BMDC samples. All 4 demonstrated reduced myeloid CFUs with increasing doses of C188-9, with a mean IC₅₀ of 2.2 μM (range, 1.9–4.9 μM). Thus, C188-9 inhibited colony formation by both normal hematopoietic

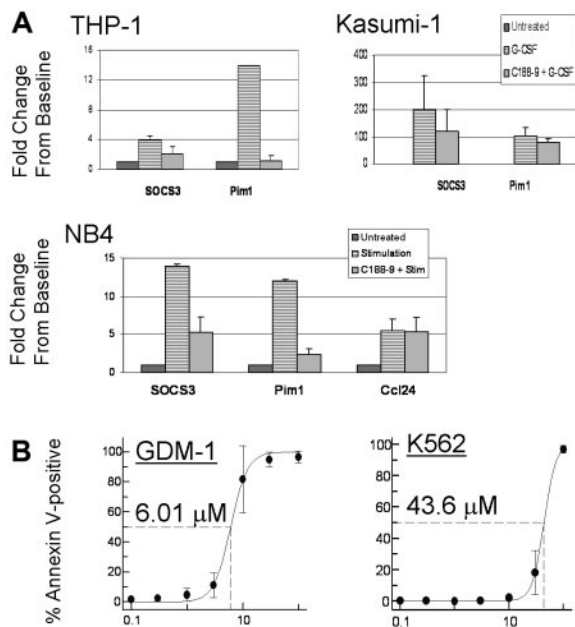


Figure 4. C188-9 inhibits G-CSF–induced expression of Stat3 target genes and induces apoptosis in AML cell lines. (A) G-CSF–induced expression of *SOCS3* and *PIM1* mRNA in 3 cell lines is shown. Cells were treated with 10 μM C188-9 for 1 hour or left untreated, and then stimulated with 100 ng/mL G-CSF for 1 hour. Fold change in mRNA level was quantified by the $\Delta\Delta C_t$ method as described in “Quantitative RT-PCR.” Values are the mean \pm SEM of at least 2 independent experiments. NB4 cells also were treated with C188-9, then stimulated with 1 μM ATRA for 1 hour, and the relative levels of the ATRA-inducible gene *CCL24* were measured. (B) C188-9 induced apoptosis in AML cell lines. Cells were treated for 24 hours with C188-9; then apoptotic cells were quantified by labeling with annexin V–PE. The baseline percentage of annexin V⁺ cells in an untreated sample was subtracted from each drug-treated sample. Dose-response curves were generated and EC₅₀ values estimated, as shown. Each value represents the mean \pm SD for at least 3 replicates.

progenitors and myeloid leukemia cells, consistent with the known role of Stat3 in both granulopoiesis and, at least in some cases, leukemogenesis.

Finally, to confirm that Stat3 activity was still effectively inhibited after 2 weeks in methylcellulose culture, we harvested the cells from methylcellulose and analyzed them for pStat3 by FACS, for 3 samples that had sufficient cell numbers. As shown in Figure 5E, pStat3 was effectively inhibited in AML cells when cultured in methylcellulose containing growth factors and C188-9, with estimated IC₅₀ values of 70 nM (#2735), 2.5 μM (#2187), and 3 μM (#3482). Taken together, our data suggest that small-molecule inhibition of Stat3 activity induces apoptosis and blocks clonogenic growth of AML cells, supporting the proposition that such an approach may be beneficial for AML patients.

Discussion

In this study, we demonstrated that Stat3 phosphorylation was both constitutive and inducible, in AML cell lines and primary pediatric AML samples. Moreover, in our cohort of AML patients, constitutive pStat3 was common in the samples with NK (5 of 8) but uncommon in the CBF samples (1 of 10). We demonstrated that a novel small-molecule inhibitor of Stat3 SH2 domain-pY peptide interaction, C188-9, inhibited G-CSF–induced Stat3 activation and Stat3-dependent gene expression. Potential therapeutic efficacy is demonstrated by our findings that C188-9 induced apoptosis in

AML cell lines and primary samples and inhibited colony formation by primary AML blasts.

The compound also reduced colony formation by normal bone marrow progenitors, suggesting that, like current chemotherapy agents, Stat3 inhibitors may cause myelosuppression in patients. On the other hand, transgenic mice lacking hematopoietic Stat3 actually manifest neutrophilia,^{20–22} possibly because of compensatory alternative pathways, so in vivo trials will be required to determine the effect of Stat3 inhibition on normal myelopoiesis.

Constitutive pY-Stat3 has been demonstrated in AML cell lines and primary samples by a variety of methods, including Western blotting, electrophoretic mobility shift assay, and immunohistochemistry. In primary AML samples, constitutive pStat3 was demonstrated by electrophoretic mobility shift assay and/or Western blot in 25% to 100% of AML patients.^{6,8,23,24} Our phosphoflow data from pediatric AML patients, in which 33% had constitutive pStat3, are consistent with these reports. The study by Irish et al²⁵ was among the first to use phosphoflow to study signaling patterns in AML. These authors demonstrated an association between potentiated pSTAT activity and chemotherapy-resistant disease. Although our cohort was not powered for multivariate analyses, it is intriguing to note that 5 of the 6 pStat3⁺ patients were in the NK group because NK patients in general have an inferior outcome compared with CBF patients. Therefore, our finding that constitutive pStat3 was more frequent in the NK patients than the CBF patients raises the possibility that pStat3 status may prove to be an important biologic and prognostic factor for the large and heterogeneous NK group of AML patients. Validation of this finding in a larger cohort of patients is currently underway.

In addition to ligand-independent pStat3, we also examined pStat3 levels in response to G-CSF stimulation. We found that 16 of 18 primary samples responded to 100 ng/mL G-CSF with an increase in pStat3 of at least 2-fold, as did 4 of 5 normal marrow samples. The magnitude of the response varied widely; and in general, the samples with high constitutive pStat3 had a lower fold-change response to G-CSF, similar to previous findings.²⁵ We further examined the issue of G-CSF sensitivity in our AML cell lines and a small cohort of primary AML samples, using 3 doses spanning 2 logs. Again, we found considerable variability in the cell lines and the primary samples; some cases responded dramatically to the 1 ng/mL dose and others were unresponsive even to 100 ng/mL. It has been suggested that the magnitude and/or sensitivity of STAT activation in response to ligand predicts the behavior of the disease. For example, a signaling pattern characterized by high levels of cytokine-dependent pSTATs was strongly associated with relapse in AML patients,²⁵ and a signaling pattern characterized by dramatically increased sensitivity of Stat5 activation by granulocyte-macrophage colony-stimulating factor was associated with poor outcome in juvenile myelomonocytic leukemia.²⁶ Our results set the stage for further studies to specifically examine Stat3 signaling in response to various doses of ligand and to correlate signaling patterns with outcome.

In addition to characterizing Stat3 signaling in AML, this study demonstrates the potential benefit of directly inhibiting Stat3 to treat AML, using a novel small-molecule Stat3 probe, C188-9. Several other groups also have been working to develop small molecules that target Stat3. Some molecules that are used as Stat3 inhibitors, such as JSI-124 and WP1066, actually block Jak kinase activity.^{19,27} Although these drugs have the advantage of being fairly potent (low micromolar IC₅₀), they only block Stat3 activation downstream of activated Jaks, leaving open the potential for Src-dependent Stat3 activation, for example. Another class of Stat3

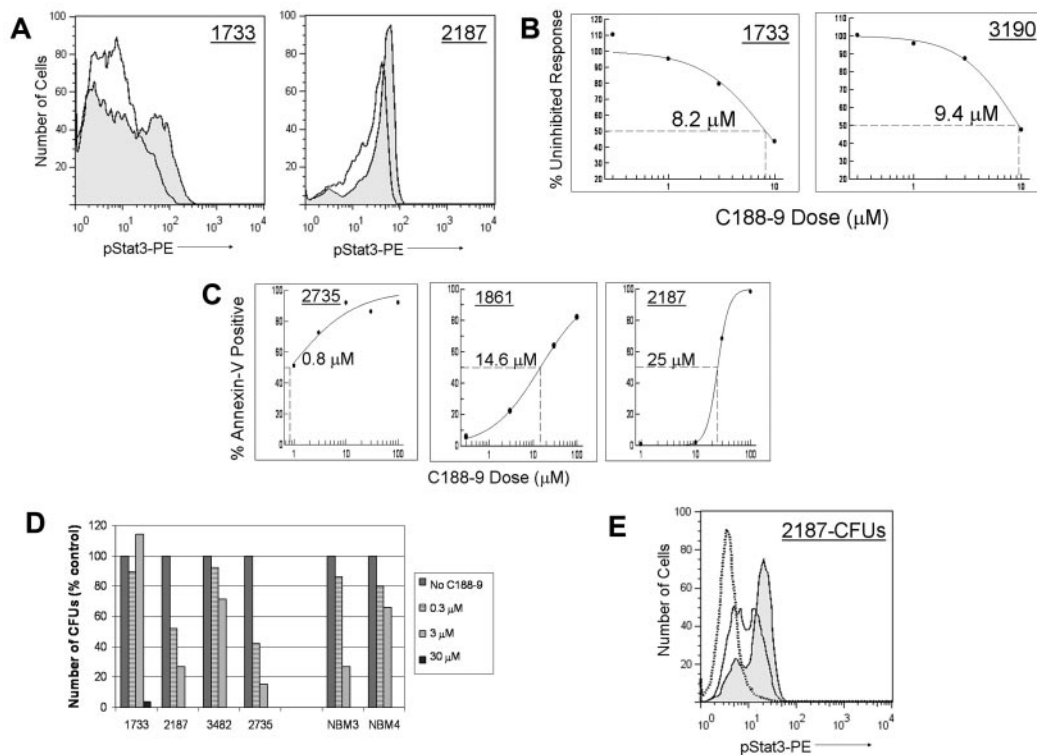


Figure 5. C188-9 inhibits G-CSF–induced pStat3, induces apoptosis, and reduces colony formation in primary pediatric AML samples. (A) C188-9 inhibited pStat3 induced by treatment with 100 ng/mL G-CSF, as shown by FACS histogram overlays. Shaded area represents G-CSF only; and solid line, G-CSF + 10 μM C188-9. (B) The percentage of the uninhibited response was determined from the MFI of the pStat3⁺ population, and dose-response curves were generated. (C) C188-9 induced apoptosis in CD34⁺ primary AML cells. Cells were incubated with C188-9 for 48 hours, and apoptosis was quantified by annexin V staining. (D) C188-9 reduced colony formation in primary AML samples grown in methylcellulose medium with growth factors. The number of colonies (≥ 30 cells; normalized to the number of colonies in untreated control dishes) in each dose of C188-9 is shown for 4 primary samples and 2 normal bone marrow samples. Sample 2187 was first plated at 1×10^5 cells/dish. After 10 days, the number of colonies in the untreated condition was too numerous to count. The untreated cells were harvested and replated in methylcellulose with increasing doses of C188-9, at 1000 cells/dish. CFUs were counted at 14 days. (E) Stat3 activation in AML cells after culture in methylcellulose with growth factors was reduced by the continuous presence of C188-9. pStat3 histogram overlays for CFUs from sample 2187 are shown. Shaded area represents without C188-9; solid line, 1 μM C188-9; and dotted line, 10 μM C188-9.

inhibitors is the peptidomimetics, which are relatively potent *in vitro*^{28,29} but historically have carried the challenge of adequate cell permeability. CPA-7, a platinum compound, has been shown to inhibit Stat3 and Stat1 activity and to reduce tumor cell growth.³⁰ This molecule, like ours, has low micromolar potency. Within the field of rationally designed, small-molecule Stat3 SH2 domain probes, we think that C188-9 compares favorably. This group of published compounds includes, though is not limited to, Stattic,³¹ STA-21,³² S3I-201,³³ LLL-3,³⁴ and LLL12.³⁵ Like C188-9, Stattic and LLL12 inhibit Stat3 activation at low micromolar doses; the other agents require higher concentrations to see measurable effects.

In almost all cases, the Stat3 inhibitors described in the preceding paragraph were characterized primarily with solid tumor cells. Our paper is among the few to describe the effects of pharmacologic Stat3 inhibition in AML. Of note, 2 recent publications reported enhanced apoptosis in K562 cells after siRNA-mediated Stat3 knockdown,^{9,36} supporting our pharmacologic approach. Just as we saw variable responses to G-CSF, we also saw variability in the responses of the AML cell lines and primary samples to C188-9. For example, although all of the cell lines had similar IC₅₀ for inhibition of G-CSF–induced Stat3 phosphorylation (4–8 μM), their EC₅₀ for apoptosis varied considerably (6–44 μM). This finding suggests that some cell lines are more dependent on (or “addicted to”) Stat3-dependent antiapoptotic gene expression than others.

Interestingly, it was not the level of constitutive pStat3, but rather the robustness of the cells’ pStat3 response to G-CSF, that

correlated with the ability of C188-9 to induce apoptosis. That is, KG-1 and K562 cells had both the smallest pStat3 responses to G-CSF and the highest EC₅₀ for apoptosis, whereas Kasumi-1 and GDM-1 cells had the largest Stat3 responses to G-CSF and were the most sensitive to apoptosis induction. This observation suggests that the phenomenon of oncogene addiction, in the case of Stat3 at least, may require a dynamic range of function, such that exogenous influences (eg, growth factors secreted by bone marrow stromal cells) can up-regulate oncogenic activity. Conversely, when the activity of an oncogene does not respond to its environment, then inhibiting its function may not significantly alter cellular behavior. Further studies are underway to determine whether there are distinct Stat3 signaling patterns in primary AML samples that can predict a greater or lesser vulnerability to Stat3 inhibition. This information may be very useful to identify those patients who probably need aggressive therapy and who would probably benefit from a drug targeting Stat3.

Acknowledgments

The authors thank Dr Soheil Meshinchi for helpful discussions.

This work was supported by the National Institutes of Health/National Heart, Lung, and Blood Institute (K08 HL085018; M.S.R.), National Institutes of Health/National Cancer Institute (P50 CA058183, R21 CA149783; D.J.T.), the CureSearch National Childhood Cancer Foundation (M.S.R.), the John S. Dunn Gulf

Coast Consortium for Chemical Genomics (D.J.T.), the Cancer Prevention and Research Institute of Texas (RP10042; M.S.R., D.J.T.), and the Dan L. Duncan Cancer Center at Baylor College of Medicine (D.J.T.).

Authorship

Contribution: M.S.R. designed and performed the experiments, analyzed the data, and wrote the manuscript; M.J.R. performed the

experiments; T.A.A. and R.B.G. provided and analyzed the clinical data and wrote the manuscript; and D.J.T. designed the experiments and wrote the manuscript.

Conflict-of-interest disclosure: The intellectual property surrounding C188 and its derivatives, including C188-9, has been licensed to StemMed Ltd, of which D.J.T. is a partner. The remaining authors declare no competing financial interests.

Correspondence: Michele S. Redell, Texas Children's Cancer Center, 6621 Fannin St, Houston, TX 77030; e-mail: mlredell@txccc.org.

References

- Wegrzyn J, Potla R, Chwaie YJ, et al. Function of mitochondrial Stat3 in cellular respiration. *Science*. 2009;323(5915):793-797.
- Yu C-L, Meyer DJ, Campbell GS, et al. Enhanced DNA-binding activity of a Stat3-related protein in cells transformed by the Src oncoprotein. *Science*. 1995;269(5220):81-83.
- Garcia R, Yu C-L, Hudnall A, et al. Constitutive activation of Stat3 in fibroblasts transformed by diverse oncoproteins and in breast carcinoma cells. *Cell Growth Differ*. 1997;8(12):1267-1276.
- Bromberg JF, Wrzeszczynska MH, Devgan G, et al. Stat3 as an oncogene. *Cell*. 1999;98(3):295-303.
- Grandis JR, Drenning SD, Chakraborty A, et al. Requirement of Stat3 but not Stat1 activation for epidermal growth factor receptor-mediated cell growth in vitro. *J Clin Invest*. 1998;102(7):1385-1392.
- Benekli M, Xia Z, Donohue KA, et al. Constitutive activity of signal transducer and activator of transcription 3 protein in acute myeloid leukemia blasts is associated with short disease-free survival. *Blood*. 2002;99(1):252-257.
- Spiekermann K, Biethahn S, Wilde S, Hiddemann W, Alves F. Constitutive activation of STAT transcription factors in acute myelogenous leukemia. *Eur J Haematol*. 2001;67(2):63-71.
- Steensma DP, McClure RF, Karp JE, et al. JAK2 V617F is a rare finding in de novo acute myeloid leukemia, but STAT3 activation is common and remains unexplained. *Leukemia*. 2006;20(6):971-978.
- Bewry NN, Nair RR, Emmons MF, Boulware D, Pinilla-Ibarz J, Hazlehurst LA. Stat3 contributes to resistance toward BCR-ABL inhibitors in a bone marrow microenvironment model of drug resistance. *Mol Cancer Ther*. 2008;7(10):3169-3175.
- Zhou J, Bi C, Janakakumara JV, et al. Enhanced activation of STAT pathways and overexpression of survivin confer resistance to FLT3 inhibitors and could be therapeutic targets in AML. *Blood*. 2009;113(17):4052-4062.
- Xu X, Kasembeli M, Jiang X, Tweardy BJ, Tweardy DJ. Chemical probes that competitively and selectively inhibit Stat3 activation. *PLoS ONE*. 2009;4(3):e4783.
- Ono M, Yu B, Hardison EG, Mastrangelo M-A, Tweardy DJ. Increased susceptibility to liver injury after hemorrhagic shock in rats chronically fed ethanol: role of nuclear factor-kappa B, interleukin 6, and granulocyte-colony stimulating factor. *Shock*. 2004;21(6):519-525.
- Chai SK, Nichols GL, Rothman P. Constitutive activation of JAKs and STATs in BCR-ABL-expressing cell lines and peripheral blood cells derived from leukemic patients. *J Immunol*. 1997;159(10):4720-4728.
- de Groot RP, Raaijmakers JAM, Lammers J-WJ, Jove R, Koenderman L. STAT5 activation by BCR-ABL contributes to transformation of K562 leukemia cells. *Blood*. 1999;94(3):1108-1112.
- Kim KT, Baird K, Ahn JY, et al. Pim-1 is up-regulated by constitutively activated FLT3 and plays a role in FLT3-mediated cell survival. *Blood*. 2005;105(4):1759-1767.
- Shirogane T, Fukada T, Muller JM, Shima DT, Hibi M, Hirano T. Synergistic roles for Pim-1 and c-Myc in STAT3-mediated cell cycle progression and anti-apoptosis. *Immunity*. 1999;11(6):709-719.
- Luesink M, Pennings JL, Wissink WM, et al. Chemokine induction by all-trans retinoic acid and arsenic trioxide in acute promyelocytic leukemia: triggering the differentiation syndrome. *Blood*. 2009;114(27):5512-5521.
- Buckley AR. Transcriptional regulation of Pim-1 by prolactin: independence of a requirement for Jak2/Stat signaling. *J Neuroimmunol*. 2000;109(1):40-46.
- Blaskovich MA, Sun J, Cantor A, Turkson J, Jove R, Sebt SM. Discovery of JSI-124 (cucurbitacin I), a selective Janus kinase/signal transducer and activator of transcription 3 signaling pathway inhibitor with potent antitumor activity against human and murine cancer cells in mice. *Cancer Res*. 2003;63(6):1270-1279.
- Lee C-K, Raz R, Gimeno R, et al. STAT3 is a negative regulator of granulopoiesis but is not required for G-CSF-dependent differentiation. *Immunity*. 2002;17(1):63-72.
- Takeda K, Clausen BE, Kaisho T, et al. Enhanced Th1 activity and development of chronic enterocolitis in mice devoid of Stat3 in macrophages and neutrophils. *Immunity*. 1999;10(1):39-49.
- Welte T, Zhang SSM, Wang T, et al. STAT3 deletion during hematopoiesis causes Crohn's disease-like pathogenesis and lethality: a critical role of STAT3 in innate immunity. *Proc Natl Acad Sci U S A*. 2003;100(4):1879-1884.
- Gouilleux-Gruart V, Gouilleux F, Desaint C, et al. STAT-Related transcription factors are constitutively activated in peripheral blood cells from acute leukemia patients. *Blood*. 1996;87(5):1692-1697.
- Schuringa J-J, Wierenga ATJ, Kruijer W, Vellenga E. Constitutive Stat3, Tyr705, and Ser727 phosphorylation in acute myeloid leukemia cells caused by the autocrine secretion of interleukin-6. *Blood*. 2000;95(12):3765-3770.
- Irish JM, Hovland R, Krutzik PO, et al. Single cell profiling of potentiated phospho-protein networks in cancer cells. *Cell*. 2004;118(2):217-228.
- Kotecha N, Flores NJ, Irish JM, et al. Single-cell profiling identifies aberrant STAT5 activation in myeloid malignancies with specific clinical and biologic correlates. *Cancer Cell*. 2008;14(4):335-343.
- Ferrajoli A, Faderl S, Van Q, et al. WP1066 disrupts Janus kinase-2 and induces caspase-dependent apoptosis in acute myelogenous leukemia cells. *Cancer Res*. 2007;67(23):11291-11299.
- Coleman DR, Ren Z, Mandal PK, et al. Investigation of the binding determinants of phosphopeptides targeted to the SRC homology 2 domain of the signal transducer and activator of transcription 3: development of a high-affinity peptide inhibitor. *J Med Chem*. 2005;48(21):6661-6670.
- Mandal PK, Limbrick D, Coleman DR, et al. Conformationally constrained peptidomimetic inhibitors of signal transducer and activator of transcription 3: evaluation and molecular modeling. *J Med Chem*. 2009;52(8):2429-2442.
- Turkson J, Zhang S, Palmer J, et al. Inhibition of constitutive signal transducer and activator of transcription 3 activation by novel platinum complexes with potent antitumor activity. *Mol Cancer Ther*. 2004;3(12):1533-1542.
- Schust J, Sperl B, Hollis A, Mayer TU, Berg T. Stattic: a small-molecule inhibitor of STAT3 activation and dimerization. *Chem Biol*. 2006;13(11):1235-1242.
- Song H, Wang R, Wang S, Lin J. A low-molecular-weight compound discovered through virtual database screening inhibits Stat3 function in breast cancer cells. *Proc Natl Acad Sci U S A*. 2005;102(13):4700-4705.
- Siddiquee K, Zhang S, Guida WC, et al. Selective chemical probe inhibitor of Stat3, identified through structure-based virtual screening, induces antitumor activity. *Proc Natl Acad Sci U S A*. 2007;104(18):7391-7396.
- Fuh B, Sobo M, Cen L, et al. LLL-3 inhibits STAT3 activity, suppresses glioblastoma cell growth and prolongs survival in a mouse glioblastoma model. *Br J Cancer*. 2009;100(1):106-112.
- Lin L, Hutzen B, Li PK, et al. A novel small-molecule, LLL12, inhibits STAT3 phosphorylation and activities and exhibits potent growth-suppressive activity in human cancer cells. *Neoplasia*. 2010;12(1):39-50.
- Ma LD, Zhou M, Wen SH, et al. Effects of STAT3 silencing on fate of chronic myelogenous leukemia K562 cells. *Leuk Lymphoma*. 2010;51(7):1326-1336.



blood[®]

2011 117: 5701-5709
doi:10.1182/blood-2010-04-280123 originally published
online March 29, 2011

Stat3 signaling in acute myeloid leukemia: ligand-dependent and -independent activation and induction of apoptosis by a novel small-molecule Stat3 inhibitor

Michele S. Redell, Marcos J. Ruiz, Todd A. Alonzo, Robert B. Gerbing and David J. Tweardy

Updated information and services can be found at:

<http://www.bloodjournal.org/content/117/21/5701.full.html>

Articles on similar topics can be found in the following Blood collections

[Editorials](#) (149 articles)

[Myeloid Neoplasia](#) (1780 articles)

[Pediatric Hematology](#) (549 articles)

Information about reproducing this article in parts or in its entirety may be found online at:

http://www.bloodjournal.org/site/misc/rights.xhtml#repub_requests

Information about ordering reprints may be found online at:

<http://www.bloodjournal.org/site/misc/rights.xhtml#reprints>

Information about subscriptions and ASH membership may be found online at:

<http://www.bloodjournal.org/site/subscriptions/index.xhtml>